의학석사 학위논문

Elucidation of morphology and characterization of the tailgut

미장의 형태학적 묘사 및 특징의 고찰

2021 년 2월

서울대학교 대학원

의학과 해부학전공

반새리

Elucidation of morphology and characterization of the tailgut

미장의 형태학적 묘사 및 특징의 고찰
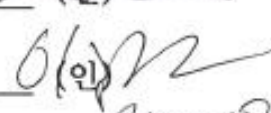
지도교수 이 지 연
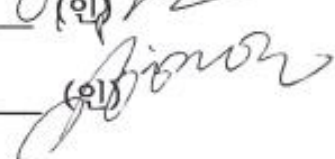
이 논문을 의학석사 학위논문으로 제출함

2020 년 10월

서울대학교 대학원

의학과 해부학전공

반새리

반새리의 석사 학위논문을 인준함

2021 년 1월

위 원 장 _____ 황영일 _____ (인)

부 위 원 장 _____ 이지연 _____ (인)

위 원 _____ 김현영 _____ (인)

2

Abstract

Elucidation of morphology and characterization of the tailgut

반새리 (Saeli Ban)

의학과 해부학 전공(Medicine, Anatomy)

The Graduate School

Seoul National University

The tailgut is an ephemeral structure located in the caudal end of the gut during the development of the GI tract. It has been noted that incomplete degeneration of the tailgut is relevant to the pathogenesis of tailgut cysts and caudal agenesis. In this thesis, to elucidate the morphology and degeneration of the tailgut, the period of degeneration is examined. The TUNEL assay demonstrated apoptosis in the tailgut, supported by basal lamina degradation, and the putative mechanisms of apoptosis induction are suggested. The results of this study may help to elucidate the normal development of the human tailgut and the pathogenesis of tailgut cysts and caudal agenesis.

Contents

List of Tables

List of Figures

Introduction

During embryonic development, the gut is elongated alongside the rostrocaudal axis, and the endoderm of the primitive gut tube ingresses through the AIP (anterior intestinal portal) and CIP (caudal (posterior) intestinal portal; Fig. 1a; an asterisk). This results in pouch-like invaginations at both ends of the gut, which later become regionalized into the foregut and hindgut. The midgut is defined as the part of the gut between the AIP and CIP that is still open to the yolk sac. In chicks, the foregut differentiates into several organs from the pharynx to the stomach, the midgut into the small intestine, and the hindgut into the large intestine, cloaca, and common gut-urogenital opening. The tailgut is known as the portion of the hindgut beyond the cloacal membranes [18], [34], [48], [46]. The cloacal membrane is derived from ectoderm and becomes perforated later in embryonic development to become the anus [3] (Fig. 1d).
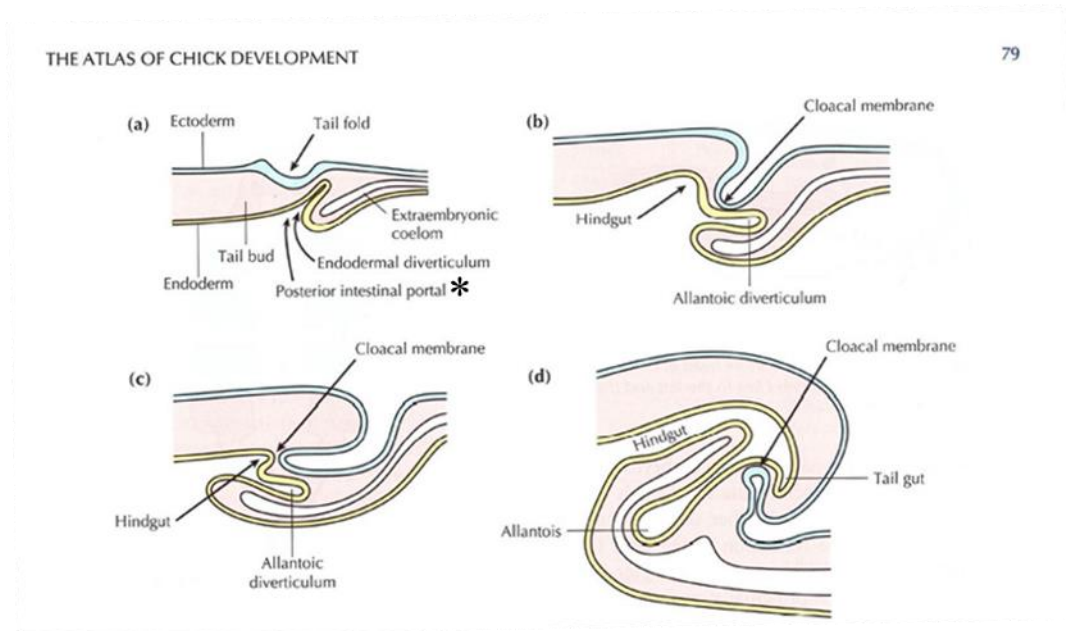
Figure 1. Formation of the tail fold, allantoic diverticulum and hindgut shown in sagittal sections at stages 12-13 (a); 13-14 (b); 18 (c); and 20 (d). With the formation of the tail fold, the cloacal membrane becomes drawn ventrally. Borrowed image from The Atlas of Chick Development (Bellaris Osmond)

The tailgut is an ephemeral endodermal tube at the most caudal part of the gut that degenerates during embryonic development. Regression of the tailgut is heralded by disintegration from the cloaca. After disconnection from the cloaca, degeneration of the tailgut progresses from the most proximal end, leaving the cloaca with a foramen. This will be closed before the end of the fourth day of incubation [3], [33], [48], [53].

It is important to study the tailgut in relation to various congenital anomalies of the posterior

body, such as tailgut cysts and caudal agenesis. The tailgut in humans is supposed to be fully degenerated by the 6th week of gestation. However, when it fails to degenerate, it remains and develops into tailgut cysts. It has been reported that nearly 50% of patients show a mass effect or pain. Resection is recommended in symptomatic cases, as it may cause inflammation or malignancy [26], [28].

Caudal agenesis is a rare anomaly (1-5 cases per 100,000) with variable levels of lower spine deformation ranging from the lower lumbar spine to the coccygeal spine. It is frequently associated with anorectal and/or urogenital malformations [12], [13], [43]. Caudal agenesis is speculated to be the result of error during secondary body formation. Primary body formation corresponds to gastrulation to form three distinct germ layers, which comprise anterior body parts from the cranial to lumbosacral level. In contrast, the secondary body is mostly derived from the tailbud, which contributes to the caudal neural tube, tailgut, notochord and so on [29], [30]. This is probably due to the common origin of the anomalous neural tube coinciding with those of the gut/urogenital organs in congenital anomalies such as caudal agenesis. Through the elucidation of the characteristics of the tailgut development, insight into the pathoembryogenesis of the related congenital anomaly may be gained.

Spatially, the tailgut is typically found dorsomedial to the tailbud, the pluripotent mesenchymal cell mass that is the main player in secondary neurulation [48]. However, as the developmental morphology of both structures is complex, the relative spatial relationship according to embryonic stages cannot be described simply. As the tailgut is the part of the gut posterior to the cloacal membrane by definition, it is located caudal to the cloacal membrane.

Although the tailgut has been described histologically using hematoxylin and eosin (H&E) staining, immunohistochemistry (IHC), electron microscopy (EM), etc., in vertebrates, including chicks, mice, rats, and humans, the focus was on the neighboring cloaca or hindgut, not the tailgut, possibly due to its underestimated biological and clinical implications because of its temporal existence and small contribution to postnatal visceral organs. It is still unclear how to distinguish the tailgut from the hindgut or cloaca and when the tailgut exists and degenerates. Additionally, the origin or role of the tailgut and the mechanism of degeneration have not been fully defined to date and remain to be elucidated.

Period of existence of the tailgut

Although the development of the tailgut and the cloaca has been shown in rodents, chick embryos are considered to be a good model that is similar to humans, as the tailgut degenerates during development. The period of existence of the tailgut in chick embryos is controversial, varying from E3 (incubation days of eggs) to E7, which corresponds to Hamilton-Hamburger stages 18-30 (HH; staged according to incubation time and morphological features) [23], [38], [48], [53], [59].

The time of the appearance of the cloacal membrane and the elongation of the hindgut and cloaca are key in determining the beginning of the tailgut. However, as the cloacal membrane and cloaca are complex structures related to the formation of the allantois by folding of the membrane, the denotation varied rather widely between reports. Hence, the real 'beginning' of the tailgut has not been concretely established, as some studies do not clarify or mention it [3] and others insist on different time points [48], [59].

Figure 2 summarizes the current literature on the appearance and disappearance of the tailgut. Romanov described that the tailgut begins to degenerate during the third day of incubation ending on day 5 (Hamburger and Hamilton (HH) stages 18 – 26) [23], [47], while Boyden observed that disintegration between the cloaca and the tailgut took place at the 41 somite stage and lasted for 12 hours (HH20-22). Concerning the completion of degeneration, Boyden described that the tailgut was removed completely during 12 hours when the final somites were formed (53-somite stage, 3 days and 18 hours), i.e., HH22. Schoenwolf [52] claimed that tailgut vestiges were observed on 8 µm-thick sagittal sections until the 6th day of incubation, while Miller and Bringlin [37] asserted that degeneration was fulfilled during the 3rd day of incubation, ending at HH22 (i.e., E3.5). Yang et al [58] also showed that degeneration of the tailgut is evident at HH22. The cavity and lining of the tailgut were reduced, and degeneration developed to the extent that the proximal end was discontinued. The degradation seemed to be completed at HH24 in that vestiges of the tailgut were observed at HH24 on sagittal sections for the last time and lasted for only approximately 36 hours.
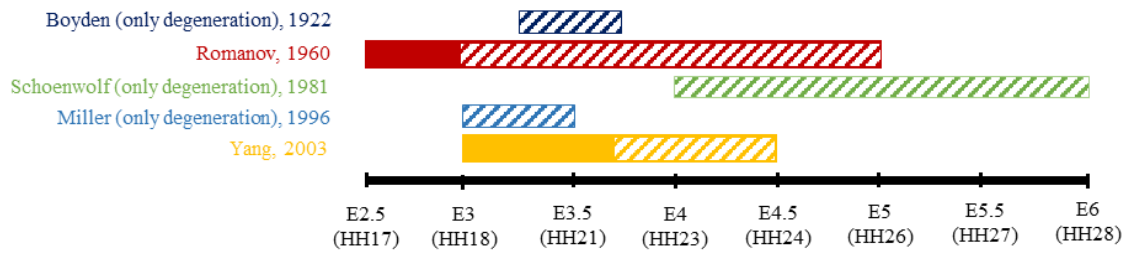
Figure 2. Summary of references arguing about the period of the tailgut appeared and degenerated according to the day of incubation (E). Historical references tend to descript embryos up to only the incubation time not the HH stage, so the timeline is based on the incubation days of eggs (E). It has been disagreed among many authors over decades. Boxes indicate when the tailgut exists and ones with diagonal line indicate when the degeneration happens.

Mechanism of degeneration of the tailgut

The mechanism of degeneration of the tailgut has been explored, which includes macrophages in phagocytosis and excludes necrosis [52]. Although Boyden observed necrotic cells during the degeneration process [3], Miller and Bringlin confirmed that apoptosis was the mechanism responsible for the degeneration, showing fragmented DNA using a TUNEL assay [37]. However, Miller and Bringlin presented only two figures in their paper, which showed some positively stained apoptotic bodies, without examination of the caudal body over other stages. Therefore, we planned to perform a TUNEL assay throughout the developmental stages with better resolution power.

To further elucidate the mechanism of tailgut degeneration, we focused on two facts from previous studies. First, in rat embryos, the tailgut is devoid of regular distribution of the basal lamina when examined using electron microscopy [17]. We sought to determine whether this was similar in chick embryos, also considering that disruption of the basal lamina is related to cell death [8].

Second, in the development of the gut, the primitive gut tube in chick embryos was reported to express Sonic hedgehong (Shh) from as early as HH13 to the newborn stages [46]. Shh signaling has been implicated in the overall developmental processes of the primitive gut [46], [47] and urogenital/anorectal organs [25], [45] as well as in neurogenesis [1], [6], [58], limb formation [1], and so on. The importance of Shh signaling in endoderm development can be inferred from the fact that Shh mutants showed anorectal malformations such as an imperforate anus [25], [35], [45]. Shh has also been shown to have an anti-apoptotic role in several contexts, especially regarding neurogenesis and cell death during development. During neurogenesis, it has been reported that neuronal cell death can be rescued by Shh-secreting cell implantation [6], and during neurulation, Shh can block its

receptor Patched (Pth) to prevent neuroepithelial apoptosis [1], [58]. Despite these implications of Shh signaling, it has not been examined in the tailgut.

Goal of the study

This study aimed to elucidate the degeneration processes of the tailgut during development. The time point of degeneration was evaluated by detailed observation of the morphology of the tailgut in chick embryos. The apoptosis was assessed by a TUNEL assay. Analysis of the basal lamina and the expression of Shh in the tailgut and related structures might reveal the mechanism of degeneration.

Materials and Method

Chick embryo sampling and processing from staining

The eggs were purchased from a local distributor of Pulmuone (Seoul, Korea) and incubated in a humidified chamber at 37℃ until the desired stages. Embryos were collected in ice-cold PBS and staged according to Hamburger and Hamilton (HH) stages (1951, Hamburger and Hamilton). Each embryo was processed, embedded in paraffin and serially sectioned at a 4 μm thickness using a sliding microtome. The slides were kept at 60℃ overnight before staining as described below.

H&E and PAS staining

The slides were deparaffinized in Neoclear (Merck, Germany), an alternative to xylene, three times for 10 minutes each. After immersion in an alcohol series with decreasing gradient concentrations, slides were washed with tap water and immersed in hematoxylin for 4 minutes, washed in tap water for 10 minutes, and then stained with eosin for 30 seconds. After dehydration with a gradually increasing alcohol series, slides were mounted with hydrophobic mounting solution. The images were taken with Tissue FAXS (TISSUEGNOSTICS).

Periodic Acid-Schiff (PAS) staining

PAS staining (Abcam, #ab150680) was performed following the distributor's instructions. Briefly, hydrated slides as mentioned above were washed in tap water, immersed in periodic acid solution for 10 minutes, rinsed with distilled water, and immersed in Schiff solution for 30 minutes to maximize the reaction. After washing in running hot tap water for 5 minutes, slides were counterstained with Mayor's hematoxylin (Dako) and mounted.

Immunohistochemistry (IHC)

The hydrated slides were microwaved in antigen unmasking solution (Vector) for 15 minutes and later cooled for 15-20 minutes. The tissues were blocked with 5% normal goat serum, 5% bovine serum albumin, and 0.5% Tween-20 in PBS for 30 minutes at room temperature. Then, tissues were incubated with anti-sonic hedgehog antibody (Santa Cruz, sc-9024) at 1:200 dilutions for 2 hours at room temperature or overnight at 4℃. After quenching endogenous signals with 3% H_2O_2 for 5 minutes, the slides were washed with PBST and incubated with biotin-conjugated goat anti-rabbit secondary antibody (Vector, #BA-1000). After incubation with ABC solution (Vector, PK-6100),

which was made 30 minutes beforehand, slides were washed with PBS, and DAB solution (Vector, SK-4100) was added for approximately 3 minutes. The reaction was stopped as soon as the color developed under a microscope. Slides were counterstained with Mayor's hematoxylin for 30 seconds, dehydrated, and mounted.

TUNEL staining

TUNEL staining was performed following the manufacturer's procedure (Sigma, s7100). Briefly, after hydration, the slides were pretreated with the protein digestion enzyme proteinase K (20 μg/mL) for 15 minutes, followed by incubation with 3% hydrogen peroxidase for 5 minutes. Subsequently, equilibrium buffer was applied for at least 10 seconds, and then, TdT enzyme was applied for an hour in a humidified chamber at 37℃ covered with plastic coverslips. After incubation, the slides were moved to a coplin jar with Stop/Wash buffer, washed with PBS, and treated with anti-digoxigenin conjugate for 30 minutes. Then, after another washing with PBS, the sections were treated with diaminobenzidine (DAP) to develop color for approximately 3 minutes, monitored under a microscope, which was stopped by washing with dH$_2$O, counterstained with Mayor's hematoxylin for 30 seconds, and mounted.

Micro-CT

Embryos were processed and imaged by computed tomography (CT). The images were reconstructed with the CT vox (version 3.0) program, by which images could be modified, such as cutting or clipping, so that internal structures could be visualized at any plane angle. The contrast or transparency of the section can be modulated using the CT vox program.

Results

1. Tailgut morphology and period of existence

To clarify the stages when the tailgut was present and the morphological changes according to the stages, caudal bodies of chick embryos were serially examined from HH16 to HH28 (Table 1).

Table 1 The number of samples examined. The "TG/ Examined (%)" column means the number of samples where tailgut was observed per the number of the chick embryos examined in the designated stages. The estimated percentages are shown in parentheses. Note the abrupt reduction at HH26.

Stage (HH)	TG / Examined (%)
16	0/5 (0)
17	6/6 (100)
18	28/28 (100)
20	44/44 (100)
22	28/28 (100)
24	29/31 (93.5)
25	5/9 (55.5)
26	5/19 (26.3)
27	1/7 (14.2)
28	0/19 (0)

The explanation of histological sections goes in the caudal-to-rostral direction unless otherwise indicated. At HH16 (n=15) (Fig. 3), the tailbud (an asterisk) was observed as a dense mesenchyme, and the endodermal allantoic diverticulum (Fig. 3a-e; dotted box) was seen as a separate lumen. The hindgut has yet to be fully developed, and the divergent lining of the endoderm (Fig. 3f-l; closed arrowhead) looked in close proximity to the notochord in the area of the midgut (Fig. 3l; arrow). Two separate cavities of the caudal neural tube (Fig. 3j, k; open arrow) were denoted, which was in contrast to the solitary cavity seen in the rostral neural tube (Fig. 3l; open arrow).

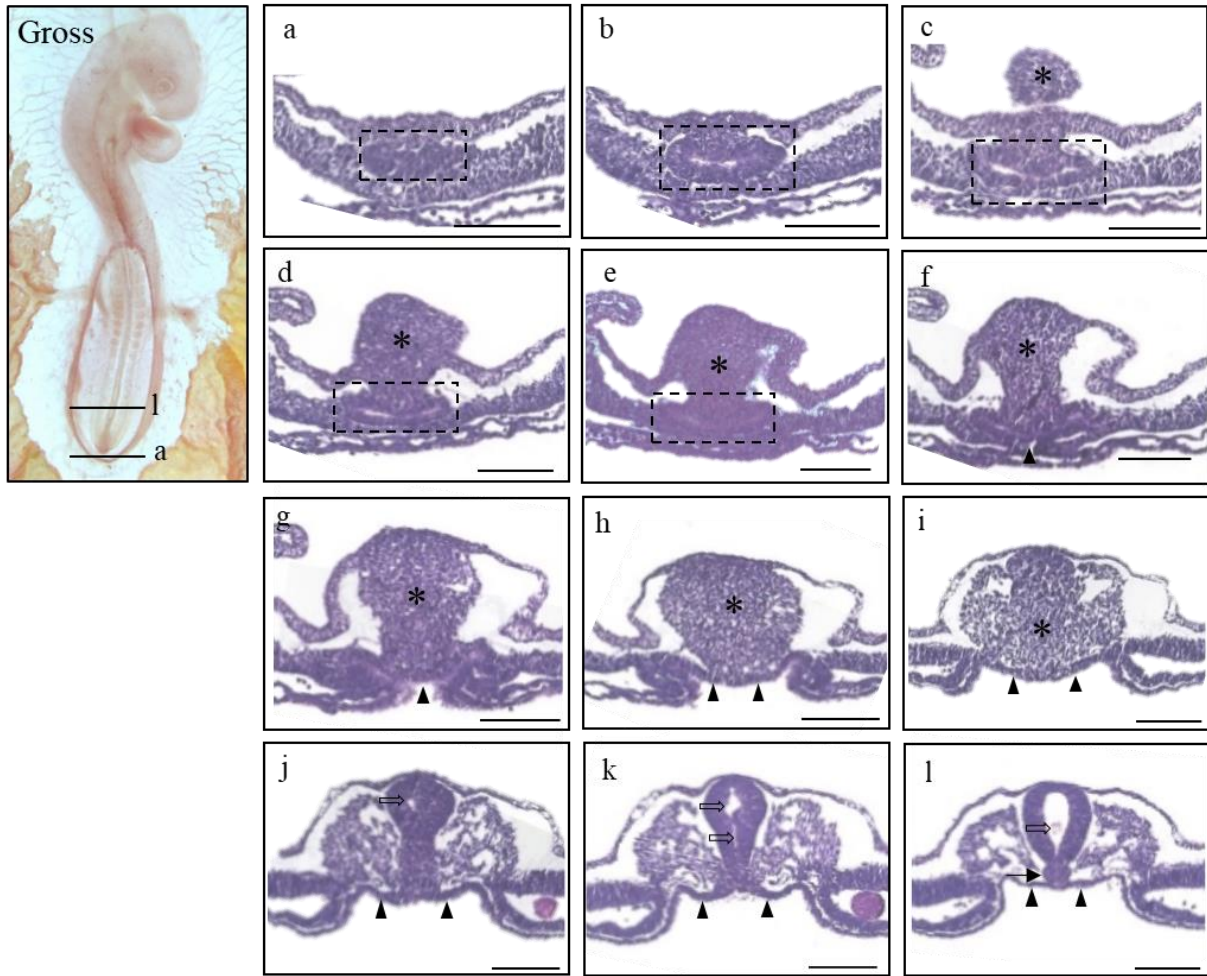Figure 3. Gross morphology of HH 16 chick embryo in the left panel (Gross) and histological sections of the stage listed in a caudal-rostral order (a)-(l). The level of sectioning is marked in the gross photo. Indications used as follows. Dotted box (a)-(e) : the allantoic diverticulum; asterisk (c)-(i) : the tailbud, open arrows : the neural tube; closed arrows : notochord. Scale bar = 100 μm.

At HH17 (n=6) (Fig. 4), the tailgut began to appear as an intact tube with a lumen for the first time at a more caudal level than the cloacal membrane (Fig. 4i; asterisk). From the caudal-most end, the convergent mass of the future tailgut and notochord (Fig. 4b; open arrowhead) can be observed as part of the tailbud. In the more cephalad sections, the mass began to look distinct with a clear margin, and it was the presumptive tailgut region (Fig 4d-h: closed arrowhead) that was located in the central area of the tailbud and ventral to the notochord (NT). The columnar epithelium of the dorsal (Fig. 4f; D) part of the tailgut became prominent, while those of the ventral (Fig. 4f; V) part seemed ambiguous and mingled with the tailbud (Fig. 4f). As the ventral ectodermal ridge (VER) (Fig. 4h; arrow), the thickening of the embryonic ectoderm on the ventral side of the tail, which is known as a critical signaling center for tail growth, became recognizable, and the thickened extraembryonic ectoderm, VER, and embryonic endoderm fused together, resulting in a cloacal membrane (Fig. 4i; asterisk). The cloacal membrane indicated the boundary between the tailgut and hindgut by definition, and thus, from here upward, the rostral gut belongs to the hindgut.

Figure 4. Gross morphology of the HH17 embryo presented on the left panel (Gross), and the histological sections listed in a caudal-rostral order (a)-(l). The level of sectioning is marked in the gross photo and a figure of Atlas is borrowed to be compared. Indications used as follows. Open arrowhead : convergent mass of the   tailgut and notochord (b); closed arrowhead : the tailgut (c)-(h); closed arrow : VER (ventral ectodermal ridge) (h); asterisk : cloacal membrane (i). Scale bar = 100 μm.

In the figure of HH18 (n=28), histological sections showed the assembled mass of the tailgut and notochord (Fig. 5b; closed arrowhead), and as the mass segregated into the notochord and tailgut, the lumen of the tailgut became apparent (Fig. 5c-g; open arrowhead) in a vertically elongated shape. However, the ventral side (Fig. 5d; closed arrow) of the tailgut was still not distinct from TB. In the more cephalad sections, with the pointed end of the dorsal side of the tailgut becoming more pointed at the dorsal side, the vertical length of the lumen shortened (Fig. 5e; open arrowhead), and eventually, the shape broadened into a more oval shape (Fig. 5f; open arrowhead). Further rostral sections showed that the lumen of the tailgut began to enlarge with the eminence of VER (Fig. 5g; open arrow). Following the appearance of VER, fusion of extraembryonic ectoderm and embryonic tissue was observed (Fig. 5h, i; asterisk), which consisted of a cloacal membrane. The cloacal membrane appeared to be a tangled rope facing the extraembryonic ectoderm. In more cephalad sections, the allantoic diverticulum was revealed by its elongated morphology (Fig. 5j), which was in continuity with the hindgut (Fig. 5l) ventral to the notochord with noticeable limb buds (Fig. 5l; indicated by "LB") laterally.
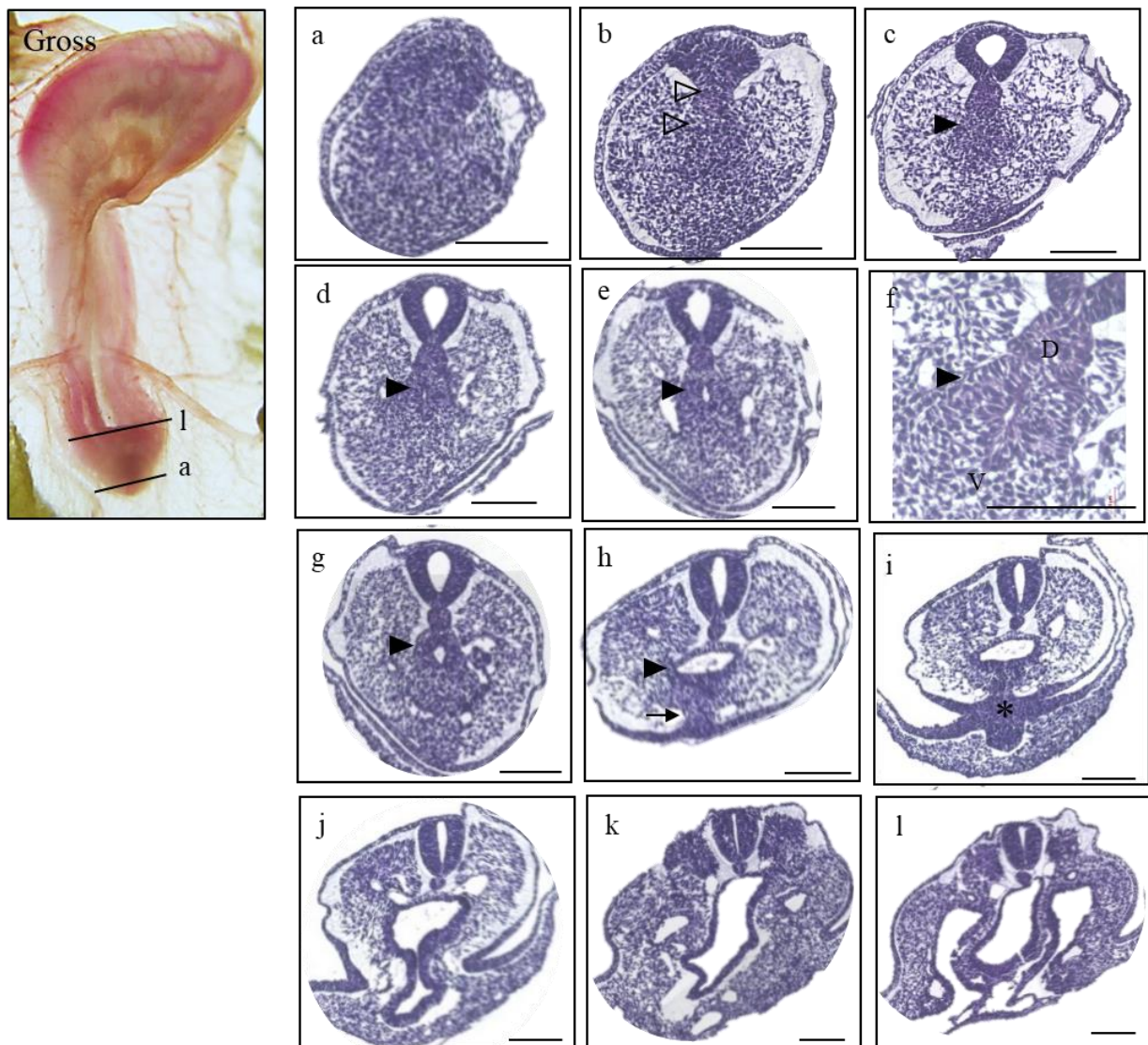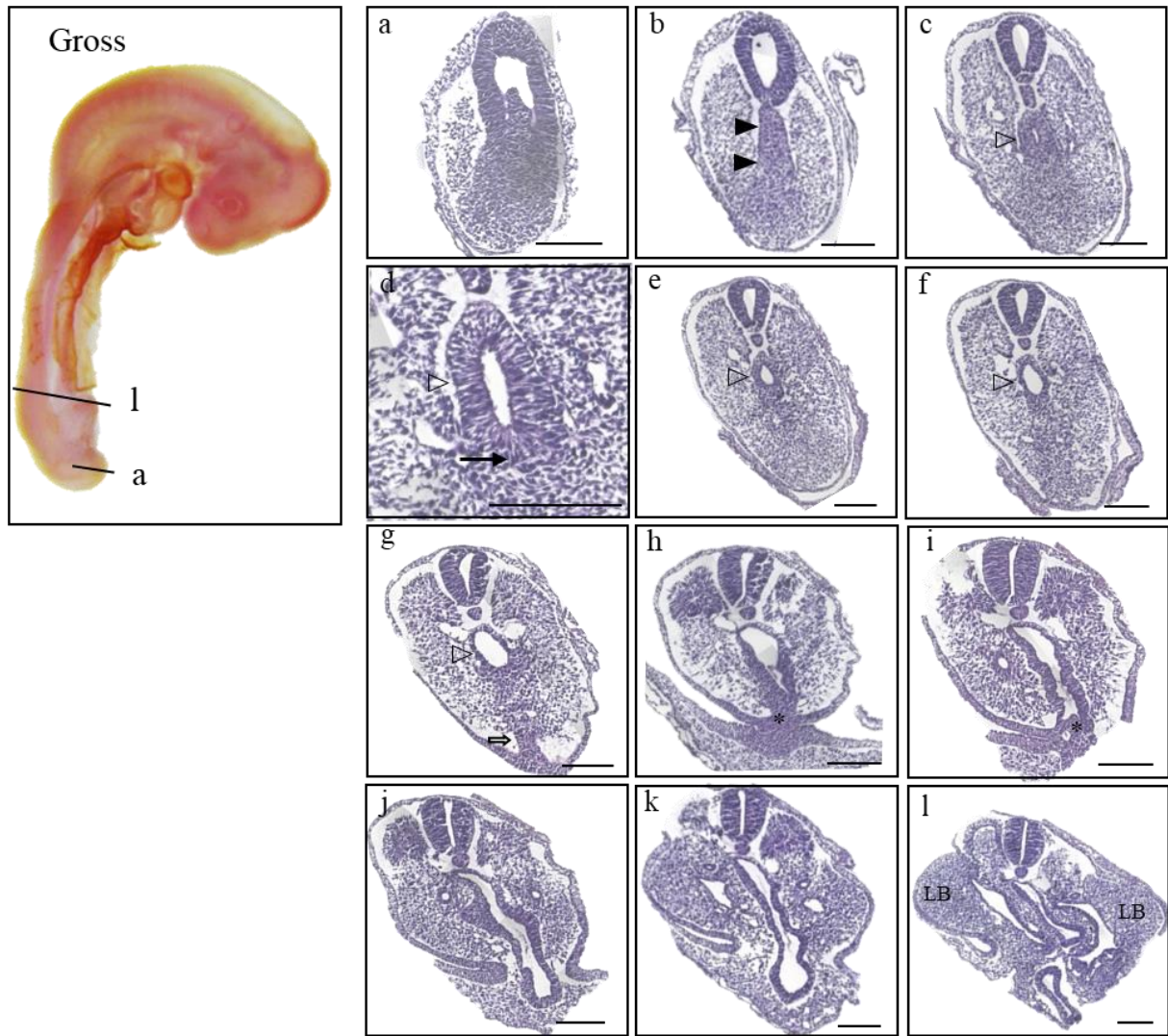
Figure 5. Gross morphology of HH18 embryo presented on the left panel, and the histological sections listed in a caudal-rostral order (a)-(l). The level of sectioning is marked in the gross photo, and a figure of Atlas is borrowed to be compared. Indications used as follows. Open arrowhead : mass of the tailgut and notochord (b); open arrowhead : the tailgut (c)-(g); closed arrow : ventral side of the tailgut (d); asterisk : cloacal membrane (h), (i); LB : limb bud (l). Scale bar = 100 μm.

At HH20 (n=44), the embryo had completely developed an allantois (Fig 6. Gross morphology; open arrow). The tailgut showed its maximum diameter in Figure 6d (closed arrowhead), and some surplus cell mass was recognized just ventral to the tailgut, which appeared to be part of the tailbud (Fig. 6d; open arrowhead). The width of the tailgut diminished to degenerating vestiges and eventually degraded completely (Fig. 6f-i; open arrowhead). The degenerating vestiges were especially marked in the midline close to the cloaca (Fig. 6g; open arrowheads). More rostrally, the cloaca was remarkably broadened and lined with the thick endoderm (Fig. 6j, k; closed arrow), and the allantois had been inflated (Fig. 6l; open arrow).
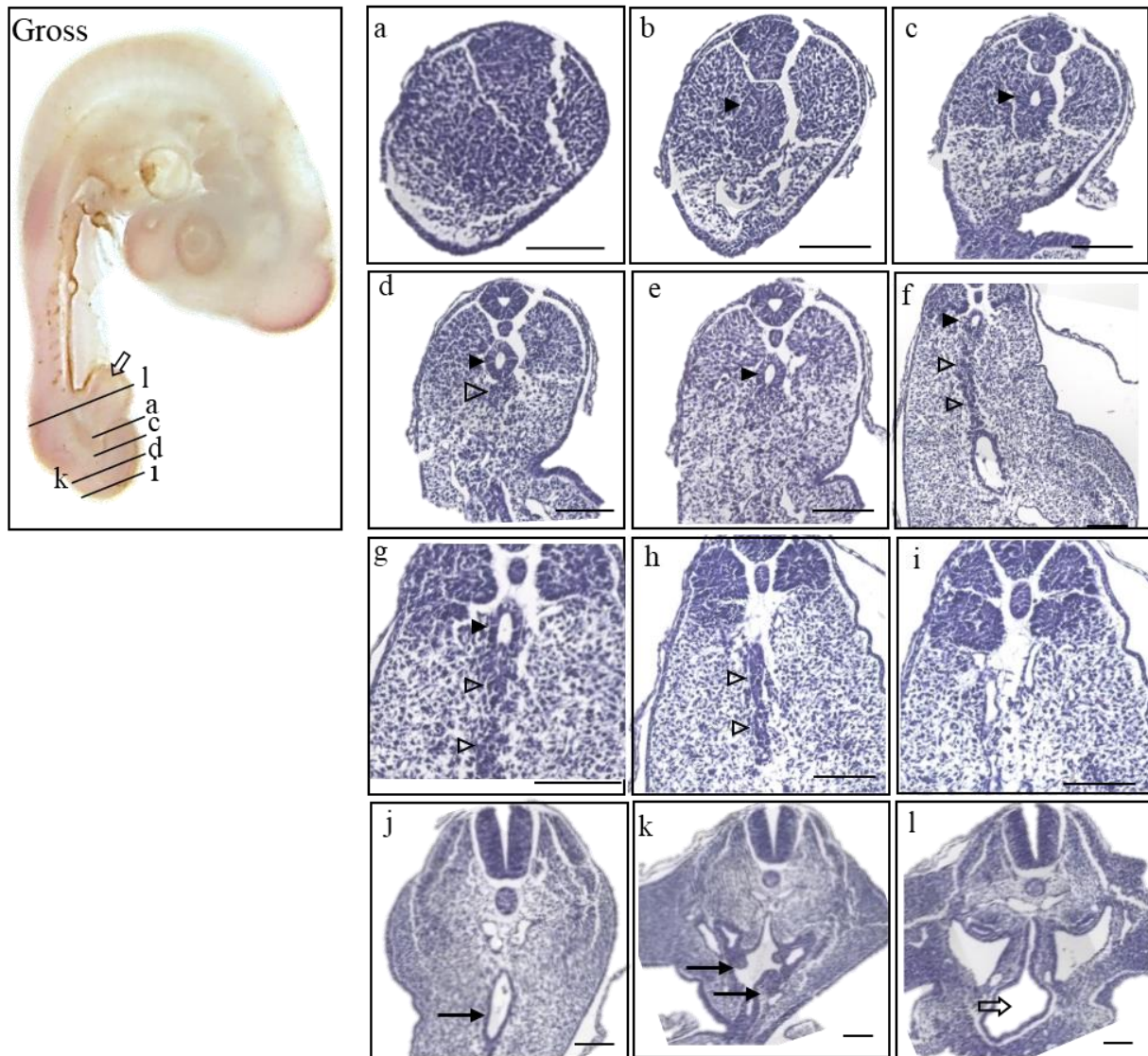
Figure 6. Gross morphology of HH 20 chick embryo in the left panel (Gross) and histological sections of the stage listed in a caudal-rostral order (a)-(l). The level of sectioning is marked in the gross photo, and a figure of Atlas is borrowed to be compared. Due to the flexure of the tail, (k) and (d) is sectioned simultaneously, as deginated on the gross photo. Note the radial arrangement of the cells in the central region of the tail bud corresponding to the presumptive tailgut in more cephalad sections (Fig. 6b; closed arrowhead). Indications used as follows. Closed arrowhead : tailgut (c)-(g) ; open arrowhead : vestiges (d)-(h) ; closed arrow : cloaca (j), (k) ; open arrow : allantois (Gross, l). Scale bar = 100 μm

As the anatomical relationship between the tailgut, hindgut, and cloaca was difficult to show in a 2D histology section, we utilized the 3D micro-CT technique. It was of use in that the 3D micro-CT image showed the exact plane of virtual sectioning. A box in Figure 7a demonstrates where the caudal body was precisely cut in Figure 7b as well as in Figure 7c for Figure 7d. On the sagittal image of an HH18 embryo, the continuation of the tailgut and hindgut was confirmed (Figure 7a, b). The tailgut (Fig. 7b; open arrowhead), posterior to the level of the cloacal membrane (Fig. 7b; closed arrowhead), was situated midline in the tailbud, which was connected through the hindgut up to the midgut and still open to the spacious yolk sac (Fig. 7b; Y).

In HH20, the discontinuation of the tailgut from the cloaca (Fig. 7c, d; arrowhead) was clearly noted in the sagittal image. This provided strong evidence that the degeneration of the tailgut progressed in a rostrocaudal direction, meaning that the proximal end of the tailgut was the first to be detached and degraded, not the distal end. The micro-CT also confirmed that towards the proximal end of the tailgut, the diameter of the tailgut increased slightly and then decreased in an abrupt manner to be diminished at the cloacal membrane level (Fig. 7d; open arrowhead), while the adjacent cloaca enlarged (closed arrows). The micro-CT images would be such great supporting data, but due to the thickness of the embryo and the limit of resolution, the embryo from the HH22 was unable to be virtually sectioned.
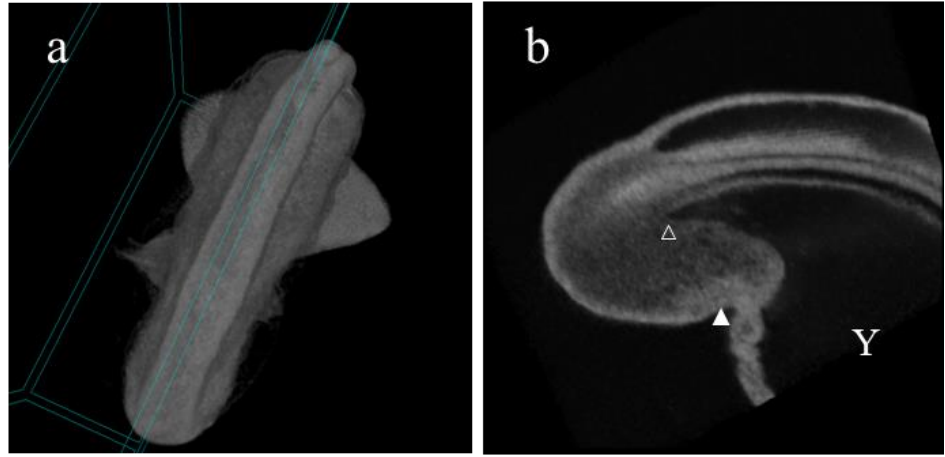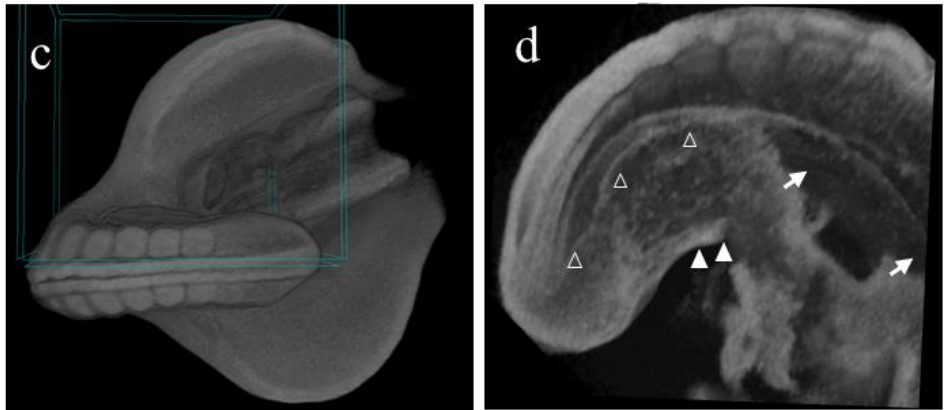
Figure 7. Micro-CT image of HH18 and HH20 embryos. The micro-CT images of (a) and (c) showed the angle of the virtual section represented on the figure (b) and (d), respectively. Indications used as follows. Open arrowhead : the tailgut (B, D) ; closed arrowhead : cloacal membrane (b, d) ; Y : yolk sac (b); closed arrow : cloaca (b).

At HH22 (n=28), the curve of the embryo was outstanding (Fig. 8; gross morphology). The diameter of the tailgut increased and then decreased towards the proximal end in a series of caudal sections (Fig. 8a-d; closed arrowhead). Notably, the tailgut appeared to be integrated into the tailbud more definitely than the earlier stages. (Fig. 8a-d; closed arrowhead). The degeneration of the tailgut was quite pronounced so that the caliber of the tailgut was barely noticeable along its AP axis and only the miniscule dot-like vestige of the tailgut persisted to the level of cloaca, just ventral to the notochord (Fig. 8e-p; open arrowhead).

Figure 8. Gross morphology of HH22 embryo presented on the left panel (Gross), and the histological sections listed in a caudal-rostral order (a)-(i). The level of sectioning is marked in the gross photo. A figure of Atlas is borrowed to be compared. Note that (a)-(f) is rather closely located, apart from (g), (h) or (i). Indications used as follows. Closed arrowhead : the tailgut (a)-(d); open arrowhead : vestiges of the tailgut (d)-(f). Scale bar = 100 μm.

At HH24 (n=31), only scarce vestiges of the tailgut were visible in a few caudal sections (Fig. 9c-f; closed arrowhead). The length of the tailgut rarely remained, which was demarcated from prior developmental stages, considering that sections intervening with the tailgut and cloaca did not show any vestiges of the tailgut (Fig. 9h-l), compared to HH22, where the vestigial dot-like tailgut was observed. The lumen was indicated to expand and shrink posteriorly, and the ventral wall was still blended with the tailbud, making it difficult to distinguish them.

Figure 9. Gross morphology of HH24 embryo presented on the left panel (Gross), and the histological sections listed in a caudal-rostral order (a)-(l). The level of sectioning is marked in the gross photo. A figure of Atlas is borrowed to be compared. Note that (a)-(g) and (h)-(j) is rather closely located, apart from (k) or (l). Indications used as follows. Closed arrowhead : the tailgut (c)-(f). Scale bar = 100 μm

At HH26 (n=19) (Fig. 10), the tailbud was denoted as a densely packed cell mass without indication of the tailgut, while only a few caudal sections appeared to have the tailgut just dorsal to the tailbud. Specifically, 5 embryos out of 13 (26%) exhibited lingering vestiges of the tailgut, and thus, general degradation was accomplished at this time point.
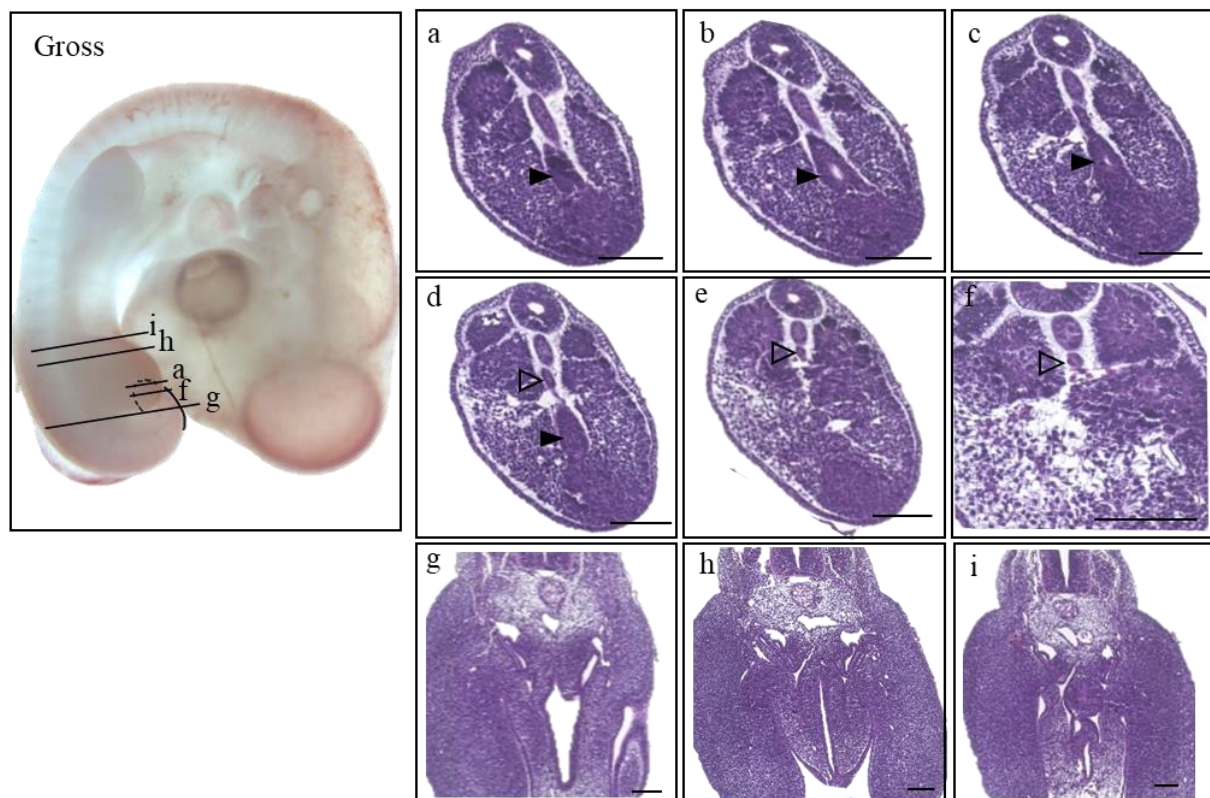

Figure 10. Gross morphology of HH26 embryo presented on the left panel (Gross), and the histological sections listed in a caudal-rostral order (a)-(k). The level of sectioning is marked in the gross photo. A figure of Atlas is borrowed to be compared. Note that (a)-(e) is rather closely located, apart from (f), (g) or (i), and that (g) and (h) are sectioned at the same time due to the fleuxure. Indications used as follows. Closed arrowhead : the tailgut (b)-(d); open arrowhead : the tailbud (a)-(c). Scale bar = 100 μm.

At HH27 (n=7), 1 embryo out of 7 (14%) showed few vestiges of the tailgut, and at HH28 (n=19), 0 out of 19 embryos showed vestiges. At HH28 (Fig. 11), 2 embryos were observed with some vestiges where the tailgut was supposed to be but without any indication of lumen with endodermal lining. In addition, HH28 did not show any persistent tailgut. These frequencies led to the conclusion that degeneration of the tailgut was already over in these stages.
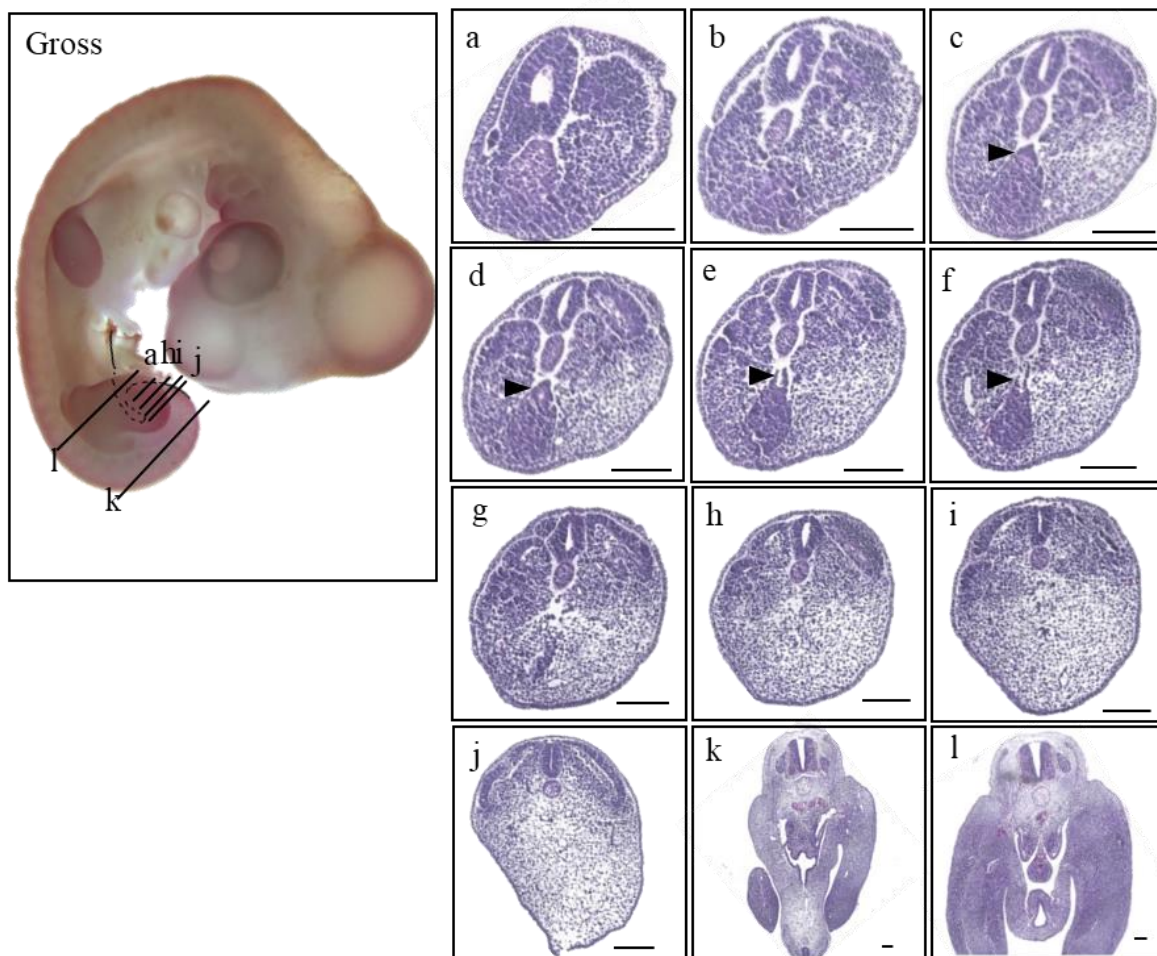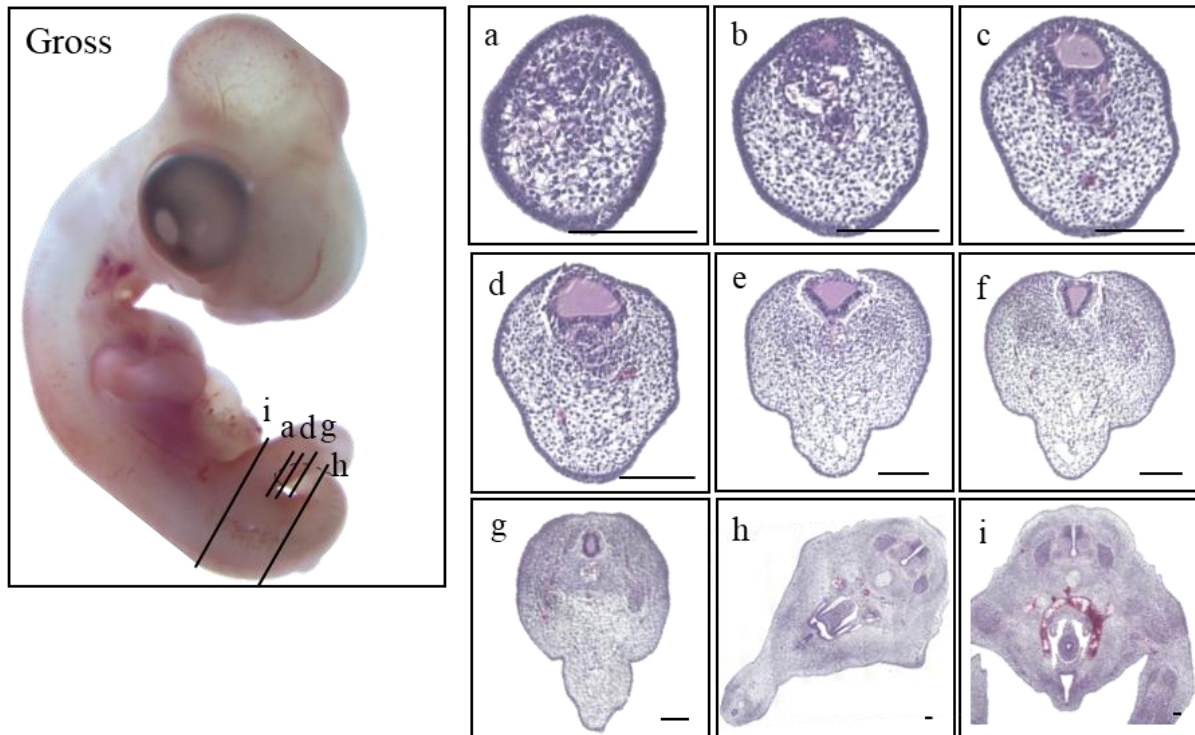

Figure 11. Gross morphology of HH28 embryo presented on the left panel (Gross), and the histological sections listed in a caudal-rostral order (a)-(i). A figure of Atlas is borrowed to be compared. The level of sectioning is marked in the gross photo. Note that (a)-(d) is rather closely located, apart from other sections. Scale bar = 100 μm.

Then, returning to HH25 was necessary to clarify the last stage of tailgut existence. At HH25 (n=9) including HH25+ which slightly outgrew but still belonged to the criteria of HH25, 5 out 6 HH25 embryos (83%) were examined to have the tailgut, and HH25+ embryos showed the tailgut with a frequency of 0 out of 3. Conclusively, the tailgut in chick embryos existed from HH17 to HH26, and degeneration was initiated from HH20 and ended at HH26.

The length of the vestiges was measured using 3 embryos for each stage. The length of the tailgut vestiges was calculated with three embryos to be 300 μm on average in HH22. Calculating the mean of three random embryos yields 11 sections, which are 43 μm long on average with a standard deviation of 18 μm in HH24. On average, of the 3 embryos randomly picked, the tailgut extends 8 serial sections, in total approximately 32 μm long, with a standard deviation of 4 μm in HH26, demonstrating the abrupt regeneration of the tailgut during development.

2. Apoptosis removes the tailgut during HH20 - HH26

The tailgut is distinguished by degeneration from its proximal end, while other parts of the primitive gut remain to be developed into multiple digestive, urogenital, or rectal organs. The mechanism of degeneration is known as apoptosis, and apoptotic figures, known as pyknotic bodies, can be detected using TUNEL staining.

In HH20 embryos, the proximal end of the tailgut was heavily stained such that multiple brownish circular specks were noted. (Fig. 12c; closed arrowheads). The apoptotic bodies were aligned in the area where the cloaca and the tailgut were separated (Fig. 12c; closed arrowheads), but apoptosis was barely detected in the distal end (Fig. 12a). This supports the idea that the degeneration of the tailgut proceeded in the rostrocaudal direction.

It seemed that the ventral part of the tailgut showed more active degeneration than the dorsal part because the apoptotic figures were concentrated mainly in the ventral region. In HH22 embryos (Fig. 12d-f), apoptotic figures were prominent at the ventral side, intermingling with the tailbud. This pattern of expression was conserved throughout HH20–HH26 (Fig. 12b-k). In contrast, only a few apoptotic bodies were present on the dorsal side (Fig. 12e, f, i)

Miller (1996) asserted that degeneration of the tailgut occurs during the 3rd day of incubation, meaning from HH20 through HH22. Unexpectedly, an advanced staining kit and resolution power enabled us to observe tailgut underset apoptosis from HH20 to HH24. Additionally, if any vestiges remained in HH26 (Fig. 12j-l), apoptotic bodies were observed. Therefore, this study showed that the degeneration of the tailgut lasted longer than previously known.
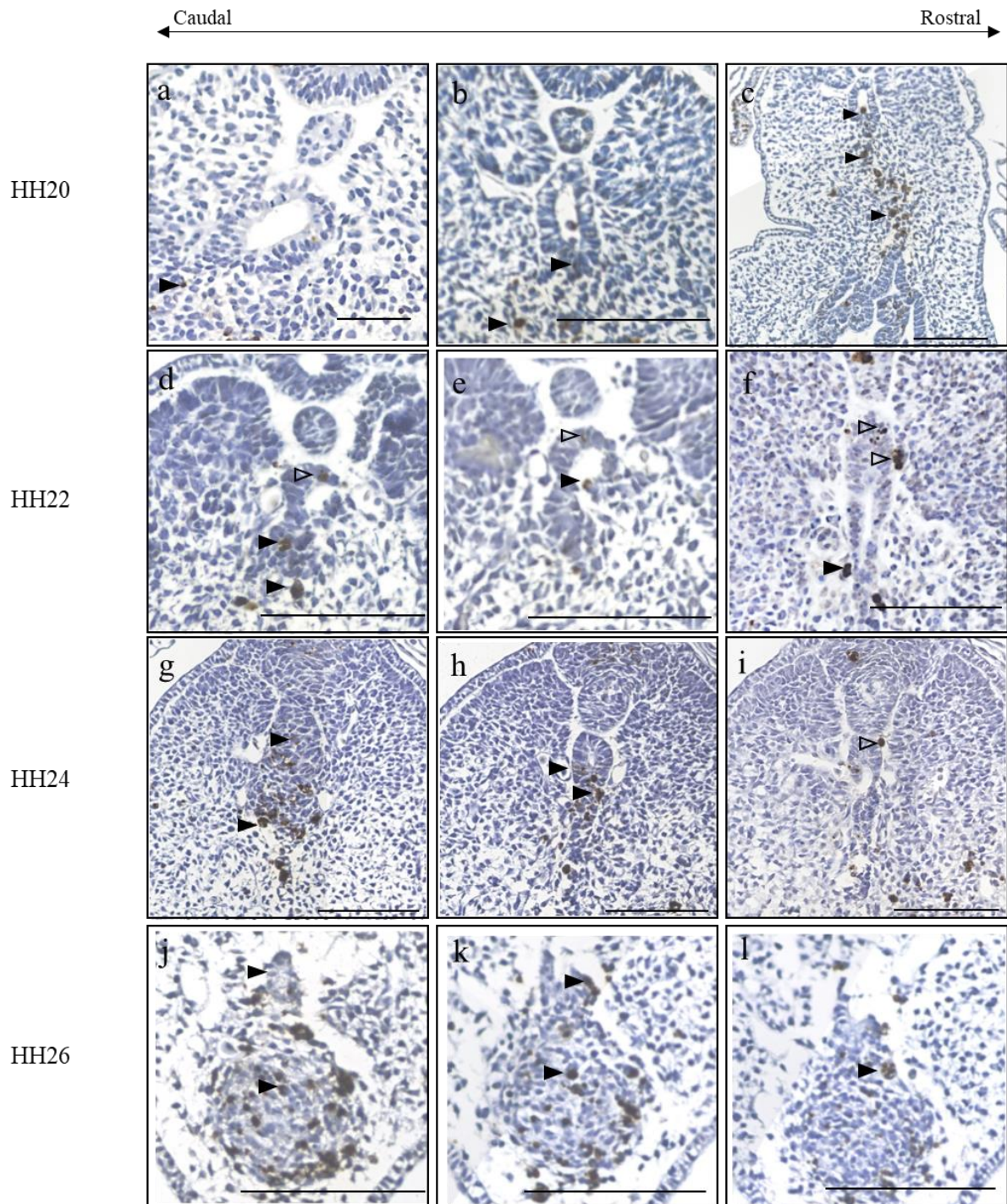
Figure 12. Apoptosis were detected by TUNEL assay in HH20 (a)-(c), HH22 (d)-(f), HH24 (g)-(i), and HH 26 (j)-(l), distinguished by the dense brownish dot-like figures. Indications used as follows. Closed arrowhead : apoptotic figures; open arrowhead : dorsal apoptotic figures(d, e, f, i). Scale bar = 100 μm.

Apoptosis and degradation of basal lamina

The tailgut has been known to have an uneven distribution of the basal lamina in its extracellular matrix (ECM) in rat embryos [13], [16], [17]. It was intriguing to determine whether the tailgut of the chick embryo represented the discontinuous basal lamina as well, which has never been examined in chick embryos thus far. To determine the basal lamina distribution, periodic acid-Schiff (PAS) staining was performed with HH20, 22, and 24 embryos with their tailgut clearly demarcated from the cloaca.

The histochemical analysis showed that the epithelium of the hindgut (Fig. 13c, f, i) and cloaca (Fig. 13b, e, h) were clearly stained, denoted with a pinkish thin lining at their basal membrane, compared to those of the tailgut (Fig. 13a, d, g) in all stages examined. In HH20 (Fig. 13a-c), even though the minute size of the tailgut restricted the resolution power, only the dorsal part of the tailgut was stained pink (Fig. 13a; indicated by arrows), while the remaining part of the lining cells seemed to lack staining or irregular distribution of the basal lamina, especially in the ventral part (Fig. 13a; indicated by arrowheads). In HH22 and HH24 (Fig. 13d-i), consistent expression of the basal lamina was hardly detectable in the tailgut (Fig. 13d, g), in contrast to the positive staining of the notochord located dorsally.
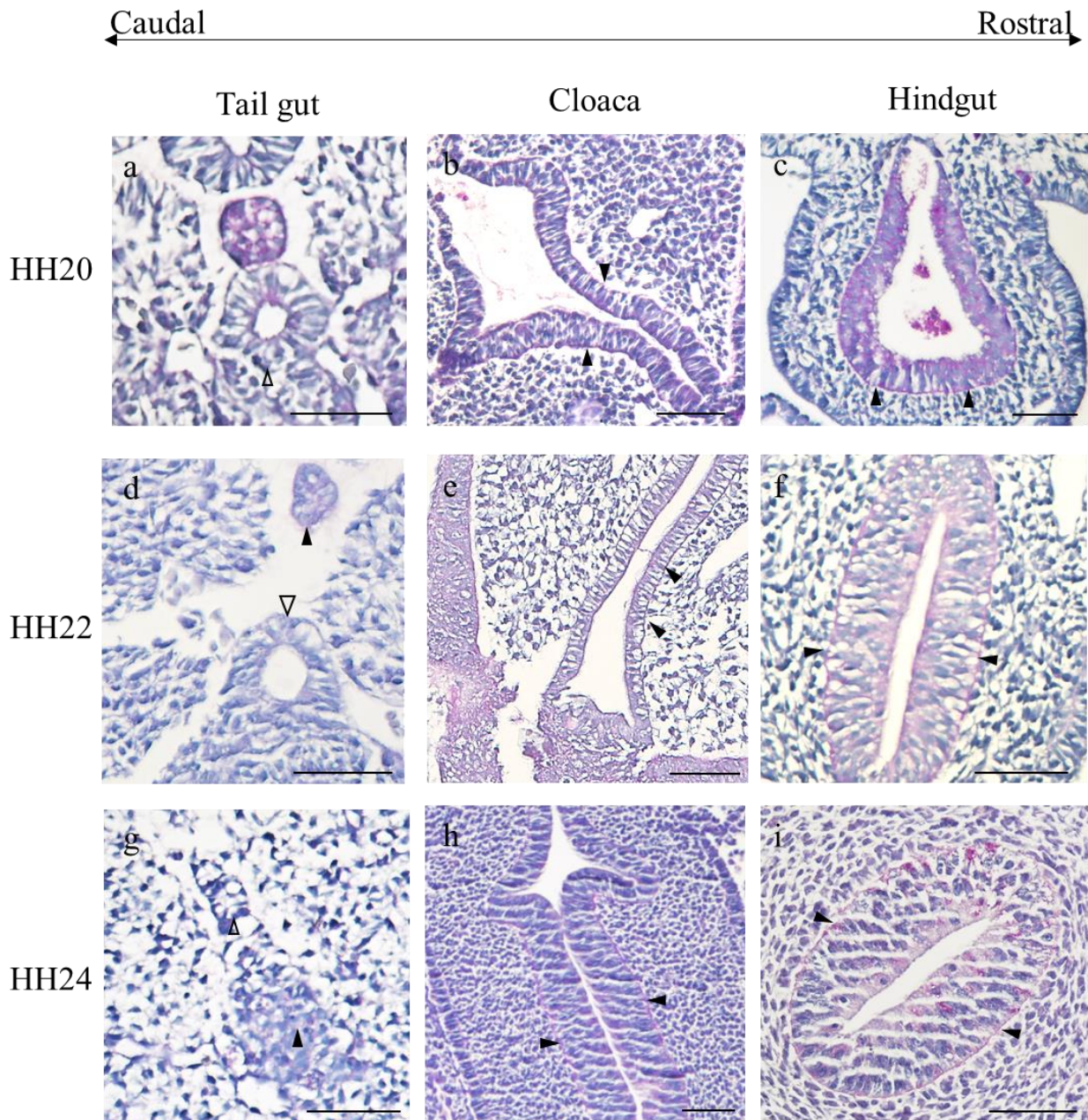
Figure 13. PAS staining shows different expression of basal lamina between tail gut in HH20 (a)-(c), HH22 (d)-(f), and HH24 (h)-(i). In each figure, closed arrowhead indicate the positively stained basal lamina, distinguished by the pinkish lining at the basal membrane of cells, while the open arrowheads indicated the irregular or absent distribution of basal lamina. Scale bar = 50 μm

3. Apoptosis may be related to the absence of sonic hedgehog (Shh) protein expression

In the development of the gut, Shh is expressed from HH13, taking part in defining the hindgut endoderm and differentiation of the cloaca, which seems to continue with the tailgut. Considering the anti-apoptotic and proliferative role of Shh, it was intriguing to determine the expression pattern of Shh in the tailgut.

As expected, the cloaca (Fig. 14e, h, k) and hindgut (Fig. 14c, f, i, l) expressed Shh, as did the floor plate of the neural tube and notochord along its anterior-posterior axis in HH18-26 embryos cells. In contrast, the caudal part of the tailgut did not express Shh in any of the stages in which the tailgut existed (Fig. 14a, d, g, j), which coincided with the region to be degraded by apoptosis. From HH18, where the tailgut becomes discernible, the tailgut does not express Shh posterior to the ventral ectodermal ridge (VER). The expression of Shh began to appear at the VER level (Fig. 14b), which was unexpected because the boundary between the hindgut and tailgut was defined as the cloacal membrane, which was located anterior to the VER. Therefore, the absence of Shh expression was shorter than expected along the AP axis. This pattern of expression persisted from HH18 to HH26.
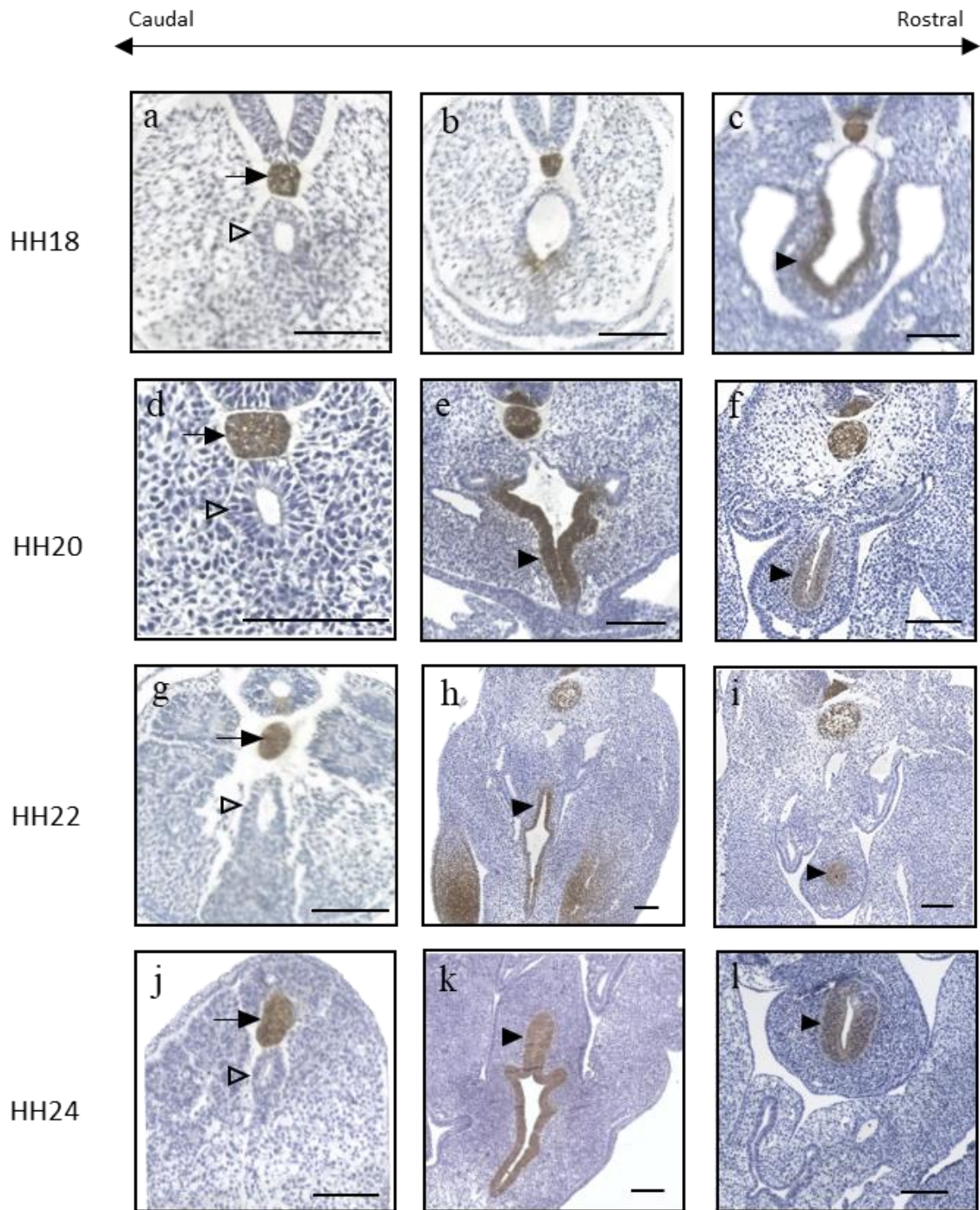
Figure 14. Patterns of Shh expression in axial sections of tail gut in HH18 (A)-(C), 20 (D)-(F), 22 (G)-(I), and 24 (J)-(L) embryos. The negative staininf of the tailgut (A, D, G, J; open arrowhead) is confimed by the expression of the nothochord (closed arrow) as an positive control. The endodermal lining of cloaca of each stage (E), (H), (K) and hindgut (C), (F), (I), (L) shows strong expression of Shh protein (closed arrowhead). Scale bar = 100 μm

Discussion

Period of the tailgut existence

Previous literature mentioned that the tailgut starts to be recognized in HH17. To clarify the period of the appearance of the tailgut, HH16 embryos were examined, and the hindgut had yet to develop. In HH17, the tailgut begins to be detected located in the central area of the tailbud and posterior to the cloacal membrane. The tailgut lumen was well defined from this stage. Of note, the ventral side of the tailgut seemed mingled with the tailbud, while the dorsal side had a distinct boundary apart from the notochord. In HH20, degeneration of the tailgut was first denoted by apoptotic pyknotic bodies at the junction of the cloaca and tailgut, namely, the cloacal membrane. The discontinuation was marked in micro-CT figures as well; in HH20, the posterior tailgut and cloaca were apart. These lingering tailgut vestiges were characteristic of HH20 onwards and marked on the ventral side rather than the dorsal side. In HH22, the discontinuation proceeded to the extent that the sections were devoid of the gut. The cloaca was denoted as crossroads, and the hindgut appeared to be a slit. For HH24, the tailgut appeared to be a part of the tailbud, and relatively, the tailbud looked larger than the tailgut. The tailgut seemed to disappear completely in HH26 (Fig. 15).
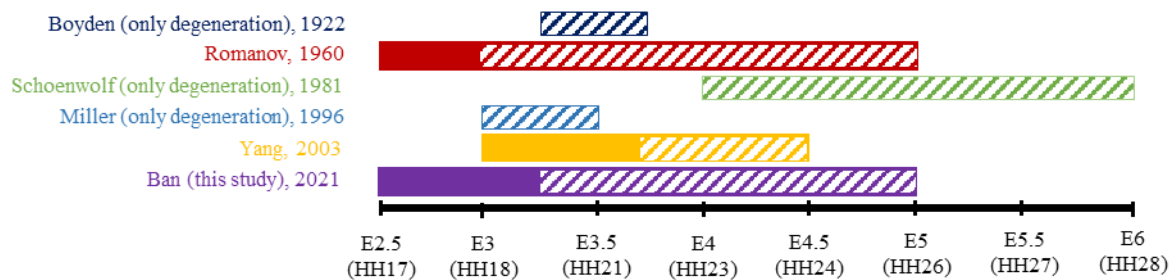
Apoptosis and degradation of basal lamina

We showed that in chick embryos, the tailgut had a discontinuous basal lamina, while the rostral hindgut and cloaca had intact basal lamina. Previous studies have provided some clues to associate the degradation of the basal lamina with the characteristic degeneration of the tailgut.

First, the irregular distribution of the basal lamina of the tailgut may be caused by anoikis.

Anoikis is apoptosis induced by hampered integrin-mediated cell adhesion and cell-ECM interactions. Attachment of a cell to the ECM can be a survival factor, and detachment can initiate an apoptotic cascade involving caspases [7], [21]. Second, cell death itself can be the cause of degradation of the basal lamina, and the phenomenon is called cataptosis. In a study evaluating degeneration of medial edge epithelial tissue during formation of the secondary palate, the authors confirmed that cell death can activate basal lamina degradation. By administering staurosporine, a cell death activator, the basal lamina of dying cells were degraded, while those of adjacent intact epithelium were unaffected [8].

Apoptosis and the absence of sonic hedgehog protein expression

Evaluation of the expression pattern of Shh in the tailgut compared to the cloaca and hindgut during development was performed based on the following: 1) Shh is expressed throughout the primitive gut from HH13 until birth; 2) Shh protein has an important role in endoderm specification and gut regionalization; 3) Shh has an anti-apoptotic role, and thus, that absence of Shh ligand can lead to an apoptotic cascade. Our results showed that the tailgut did not express Shh, while the other remaining parts of the hindgut, cloaca, and allantois did. Additionally, the dorsal part of the caudal tailgut does not express Shh, which might be caused by suppression of notochordal signaling, similar to the development of the pancreas [27], which originates from the midgut. This suppression enables the expression of pancreatic genes such as Pdx1 and insulin. This suggests the possibility of the absence of Shh playing an important role in the development of the caudal gut development, considering that both occur at the early stage of development of the primitive gut.

The importance of Shh signaling during the development of the gut and genitourinary tract can be inferred from numerous Shh mutant embryos as well as from the expression and reciprocal interaction between endoderm-derived Shh and mesoderm-derived signals such as Bmp-4 and Hoxd 13 in the gut [46], [47]. Ramalho-Santos et al generated a Shh mutant mouse strain, which appeared to have several gut malformations, such as gut malrotation with a less developed smooth muscle layer and imperforate anus, which is a major accompanying symptom of caudal agenesis in humans [45]. Liu et al showed that overexpression of Gli2, the downstream transcription regulator of Shh, induced the expression of Bmp4, Ptch, and Hoxd13, upregulated cell proliferation, and reduced apoptosis [35]. Additionally, the upregulation of p63 was detected, suggesting the interaction of the Shh and p63 pathways.

Shh has been noted to have an anti-apoptotic role and contribute to the proliferation of cells

[6]. When the neural tube and associated neural structure were extirpated, neurogenesis was hampered, and cell death increased. Then, Shh-secreting notochords and Shh-secreting fibroblasts were implanted, which all rescued the expression of Shh and apoptotic death. Additionally, it has been reported that Shh secreted from the notochord can block the induction of apoptosis by binding to its receptor Ptch, which in the absence of Shh can induce apoptosis in neuroepithelial cells [58]. As a dependence receptor, the depletion of the trophic factor Shh could induce apoptosis, where caspase-3 cleaves the intracellular domain of Ptch and then the DRAL-caspase 9 complex binds to Ptch to initiate the apoptotic cascade [37].

This anti-apoptotic function of Shh during development suggests that apoptosis of the tailgut might be related to the coinciding absence of Shh expression and the downstream signaling cascade. Considering the notochordal secretion of Shh right dorsal to the tailgut, there must be an upstream inhibitory mechanism for Shh signaling. Further study on the inhibitory mechanism of Shh signaling and the expression pattern of downstream players will be needed to determine its relevance to the induction of apoptosis.

Origin of the tailgut: separate from the hindgut

The origin of the tailgut is controversial. A dominant theory suggests that the tailgut originates from the tailbud. Along with Holmdahl, Zwilling [60] described that the tailgut (referred as the caudal intestine in the paper) is largely continued by additions from the undifferentiated tailbud, claiming different origin of the tailgut from hindgut or the rostral part of the primitive gut. Gajovic et al [17] implemented a study on the tailgut in rat embryos as well and asserted that intermingled phenotype on the ventral side of the tailgut such as in HH18 in chicks is the evidence that the tailgut is derived from tailbud through the mechanism of the mesenchymal-epithelial transition due to the absence of a distinct boundary to distinguish them, which coincides in chick embryos as well. Although limited, the results of this study also imply that at least the molecular characteristics of the tailgut are different from those of the hindgut, supporting other authors' observations [2], [9], [16], [17], [20], [29], [55], [60].

In contrast, there has been disagreement on the pluripotency of tailbud to differentiate into any germ layer, especially the potency to differentiate into endoderm. In other words, the tailbud may not have the potential to form the tailgut. In 1977, Schoenwolf performed a convincing experiment in which tailbud cells labeled with tritiated thymidine were grafted into host chick

embryos, which in the following series of developments showed that the labeled cells comprised the caudal neural tube, somites, mesenchyme, and caudal arteries, not the tail notochord, skin ectoderm, hindgut, or tailgut [50]. Additionally, Catala et al confirmed the results of Schoenwolf by graft experiments with a defined area of tail bud graft. However, in this study, the endodermal layer ventral to the tailbud was excluded from the tailbud graft, and thus, the origin of the tailgut is not conclusive [5]. Furthermore, in 1979, Schoenwolf also observed how the tailgut is formed from the endoderm located ventrally to the tailbud and not from the tailbud itself using light microscopy and electron microscopy [52]. The cell tracking experiment using several vital dyes in chick embryos suggests that the tailgut endodermal lining developed by the elongation of the hindgut, and when the movement of hindgut cells was blocked, the caudal gut failed to develop properly, even though the results in the tailgut were not specifically presented [41].

It is still controversial whether the tailgut is formed by a different process other than that of the cloaca. In other words, it still needs to be clarified whether the tailbud has the potency to develop endodermal lineages. Considering the remarkably distinct molecular characteristics of the tailgut, the tailgut may have different origins. This difference may also be induced by the interaction of the tailgut with tailbud cells after initial development because the reciprocal interaction between the endoderm and abutting mesoderm is commonly involved in gut development. Further study as to the origin of the tailgut needs to be refined, such as examination of the tailbud for the endodermal marker expression denoted in the early endoderm specification as in gastrulation [57].

Human tailgut: clinical implication

The tailgut in the human fetus has been reported to appear at Carnegie stages 10-11, which is gestational week 4, when the fetus is 3.5 mm long. Degeneration is known to be completed by stages 15-16 (gestational week 6). During existence, the caudal end of multiple structures converges into a solid mass, coined "residual mass", which looks similar to the tailbud in chick embryos [11], [18]. The degeneration process where the proximal end of the tailgut is first degraded along the anteroposterior axis with vestiges remaining at the caudal end is similar to that of chick embryos. Based on this similarity between humans and chick embryos, the study of the tailgut in chick embryos can be applied to understand the pathogenesis of tailgut cysts and caudal agenesis in humans. For instance, experiments with the inhibition of apoptosis by administering caspase inhibitors can be attempted to determine whether any anorectal or urogenital anomalies are formed.

Reference

1. Aoto K, Nishimura T, Eto K, Motoyama J. Mouse gli3 regulates fgf8 expression and apoptosis in the developing neural tube, face, and limb bud. Dev Biol. 2002;251(2):320-32.
2. Bellairs R, Osmond M. Atlas of chick development: Elsevier; 2005.
3. Boyden EA. The development of the cloaca in birds, with special reference to the origin of the bursa of fabricius, the formation of a urodaeal sinus, and the regular occurrence of a cloacal fenestra. American Journal of Anatomy. 1922;30(2):163-201.
4. Catala M. Genetic control of caudal development. Clinical Genetics. 2002;61(2):89-96.
5. Catala M, Teillet M-A, Le Douarin NM. Organization and development of the tail bud analyzed with the quail-chick chimaera system. Mechanisms of Development. 1995;51(1):51-65.
6. Charrier JB, Lapointe F, Le Douarin NM, Teillet MA. Anti-apoptotic role of sonic hedgehog protein at the early stages of nervous system organogenesis. Development. 2001;128(20):4011-20.
7. Coucouvanis E, Martin GR. Signals for death and survival: A two-step mechanism for cavitation in the vertebrate embryo. Cell. 1995;83(2):279-87.
8. Cuervo R, Covarrubias L. Death is the major fate of medial edge epithelial cells and the cause of basal lamina degradation during palatogenesis. Development. 2004;131(1):15-24.
9. DE H. Die erste entwicklung des körpers bei den vögeln und säugetieren, inkl. Dem menschen, besonders mit rücksicht auf die bildung des rückenmarks, des zöloms und der entodermalen kloake nebst einem exkurs über die entstehung der spina bifida in der lumbosakral region ii-v. Gegenbaurs Morph Jahrb. 1925;54:333-84.
10. de Santa Barbara P, Roberts DJ. Tail gut endoderm and gut/genitourinary/tail development: A new tissue-specific role for hoxa13. Development. 2002;129(3):551-61.
11. Dias MS, Azizkhan RG. A novel embryogenetic mechanism for currarino's triad: Inadequate dorsoventral separation of the caudal eminence from hindgut endoderm. Pediatric neurosurgery. 1998;28(5):223-9.
12. Duhamel B. From the mermaid to anal imperforation: The syndrome of caudal regression. Arch Dis Child. 1961;36(186):152-5.
13. Estin D, Cohen AR. Caudal agenesis and associated caudal spinal cord malformations. Neurosurgery Clinics of North America. 1995;6(2):377-91.
14. Fernandes-Silva H, Correia-Pinto J, Moura RS. Canonical sonic hedgehog signaling in early lung development. J Dev Biol. 2017;5(1):3.
15. Gajovic S, Kostović-Knežević L. Ventral ectodermal ridge and ventral ectodermal groove: Two distinct morphological features in the developing rat embryo tail. Anatomy and embryology. 1995;192(2):181-7.
16. Gajović S, Kostović-Knežević L, Švajger A. Origin of the notochord in the rat embryo tail. Anatomy and embryology. 1989;179(3):305-10.
17. Gajović S, Kostović-Knežević L, Švajger A. Morphological evidence for secondary formation of the tail gut in the rat embryo. Anatomy and Embryology. 1993;187(3):291-7.
18. GIUS JA, STOUT AP. Perianal cysts of vestigial origin. Archives of Surgery. 1938;37(2):268-87.
19. Goldman DC, Martin GR, Tam P. Fate and function of the ventral ectodermal ridge during mouse tail development. Development. 2000;127(10):2113-23.
20. Griffith CM, Wiley MJ, Sanders EJ. The vertebrate tail bud: Three germ layers from one tissue. Anatomy and Embryology. 1992;185(2):101-13.
21. Grossmann J. Molecular mechanisms of "detachment-induced apoptosis—anoikis". Apoptosis. 2002;7(3):247-60.
22. Grüneberg H. A ventral ectodermal ridge of the tail in mouse embryos. Nature. 1956;177(4513):787-8.
23. Hamburger V, Hamilton HL. A series of normal stages in the development of the chick embryo. Journal of morphology. 1951;88(1):49-92.
24. Handrigan GR. Concordia discors: Duality in the origin of the vertebrate tail. Journal of anatomy. 2003;202(3):255-67.
25. Haraguchi R, Mo R, Hui C, Motoyama J, Makino S, Shiroishi T, et al. Unique functions of sonic hedgehog signaling during external genitalia development. Development. 2001;128(21):4241-50.
26. Haydar M, Griepentrog K. Tailgut cyst: A case report and literature review. Int J Surg Case Rep. 2015;10:166-8.
27. Hebrok M, Kim SK, Melton DA. Notochord repression of endodermal sonic hedgehog permits pancreas development. Genes & development. 1998;12(11):1705-13.
28. Hjermstad BM, Helwig EB. Tailgut cysts: Report of 53 cases. American Journal of Clinical Pathology. 1988;89(2):139-47.
29. Holmdahl D. Experimentelle untersuchungen über die lage der grenze zwischen primärer und

sekundärer körperentwicklung beim huhn. Anat Anz. 1925;59:393-6.

30.	Holmdahl DE. Die erste entwicklung des körpers bei den vögeln und säugetieren, inkl. Dem menschen, besonders mit rücksicht auf die bildung des rückenmarks, des zöloms und der entodermalen kloake nebst einem exkurs über die entstehung der spina bifida in der lumbosakralregion. I. Gegenbaurs Morphol Jahrb. 1925;54:333-84.

31.	Kanki JP, Ho RK. The development of the posterior body in zebrafish. Development. 1997;124(4):881-93.

32.	Knezevic V, De Santo R, Mackem S. Continuing organizer function during chick tail development. Development. 1998;125(10):1791-801.

33.	Lillie FR. The development of the chick; an introduction to embryology: New York, H. Holt and company; 1919.

34.	LILLIE FR. Lillie's development of the chick. An introduction to embryology. New York: Holt, Rinehart and Winston; 1965.

35.	Liu G, Moro A, Zhang JJ, Cheng W, Qiu W, Kim PC. The role of shh transcription activator gli2 in chick cloacal development. Developmental biology. 2007;303(2):448-60.

36.	Lopez-Escobar B, De Felipe B, Sanchez-Alcazar JA, Sasaki T, Copp AJ, Ybot-Gonzalez P. Laminin and integrin expression in the ventral ectodermal ridge of the mouse embryo: Implications for regulation of bmp signalling. Developmental Dynamics. 2012;241(11):1808-15.

37.	Mille F, Thibert C, Fombonne J, Rama N, Guix C, Hayashi H, et al. The patched dependence receptor triggers apoptosis through a dral-caspase-9 complex. Nat Cell Biol. 2009;11(6):739-46.

38.	Miller SA, Briglin A. Apoptosis removes chick embryo tail gut and remnant of the primitive streak. Developmental Dynamics. 1996;206(2):212-8.

39.	Mills CL, Bellairs R. Mitosis and cell death in the tail of the chick embryo. Anatomy and Embryology. 1989;180(3):301-8.

40.	Mo R, Kim JH, Zhang J, Chiang C, Hui CC, Kim PC. Anorectal malformations caused by defects in sonic hedgehog signaling. Am J Pathol. 2001;159(2):765-74.

41.	Nerurkar NL, Lee C, Mahadevan L, Tabin CJ. Molecular control of macroscopic forces drives formation of the vertebrate hindgut. Nature. 2019;565(7740):480-4.

42.	Ohta S, Suzuki K, Tachibana K, Tanaka H, Yamada G. Cessation of gastrulation is mediated by suppression of epithelial-mesenchymal transition at the ventral ectodermal ridge. Development. 2007;134(24):4315-24.

43.	Pang D. Sacral agenesis and caudal spinal cord malformations. Neurosurgery. 1993;32(5):755-79.

44.	Qi BQ, Beasley SW, Williams AK, Frizelle F. Apoptosis during regression of the tailgut and septation of the cloaca. Journal of Pediatric Surgery. 2000;35(11):1556-61.

45.	Ramalho-Santos M, Melton DA, McMahon AP. Hedgehog signals regulate multiple aspects of gastrointestinal development. Development. 2000;127(12):2763-72.

46.	Roberts DJ, Johnson RL, Burke AC, Nelson CE, Morgan BA, Tabin C. Sonic hedgehog is an endodermal signal inducing bmp-4 and hox genes during induction and regionalization of the chick hindgut. Development. 1995;121(10):3163-74.

47.	Roberts DJ, Smith DM, Goff DJ, Tabin CJ. Epithelial-mesenchymal signaling during the regionalization of the chick gut. Development. 1998;125(15):2791-801.

48.	Romanoff AL. The avian embryo, structural and functional development. New York: Macmillan; 1960.

49.	Sanders EJ, Khare MK, Ooi VC, Bellairs R. An experimental and morphological analysis of the tail bud mesenchyme of the chick embryo. Anatomy and Embryology. 1986;174(2):179-85.

50.	Schoenwolf GC. Tail (end) bud contributions to the posterior region of the chick embryo. Journal of Experimental Zoology. 1977;201(2):227-45.

51.	Schoenwolf GC. Effects of complete tail bud extirpation on early development of the posterior region of the chick embryo. The Anatomical Record. 1978;192(2):289-95.

52.	Schoenwolf GC. Histological and ultrastructural observations of tail bud formation in the chick embryo. The Anatomical Record. 1979;193(1):131-47.

53.	Schoenwolf GC. Morphogenetic processes involved in the remodeling of the tail region of the chick embryo. Anatomy and Embryology. 1981;162(2):183-97.

54.	Schoenwolf GC, Delongo J. Ultrastructure of secondary neurulation in the chick embryo. American Journal of Anatomy. 1980;158(1):43-63.

55.	Svajger A. Morphogenetic features in the tail region of the rat embryo. International Journal of Developmental Biology. 2002;35(3):191-5.

56.	Švajger A, Kostović-Knežević L, Bradamante Ž, Wrischer M. Tall gut formation in the rat embryo. Wilhelm Roux's archives of developmental biology. 1985;194(7):429-32.

57.   Tada S, Era T, Furusawa C, Sakurai H, Nishikawa S, Kinoshita M, et al. Characterization of mesendoderm: A diverging point of the definitive endoderm and mesoderm in embryonic stem cell differentiation culture. Development. 2005;132(19):4363-74.

58.   Thibert C, Teillet M-A, Lapointe F, Mazelin L, Le Douarin NM, Mehlen P. Inhibition of neuroepithelial patched-induced apoptosis by sonic hedgehog. Science. 2003;301(5634):843-6.

59.   Yang HJ, Wang KC, Chi JG, Lee MS, Lee YJ, Kim SK, et al. Neural differentiation of caudal cell mass (secondary neurulation) in chick embryos: Hamburger and hamilton stages 16-45. Brain Res Dev Brain Res. 2003;142(1):31-6.

60.   Zwilling E. Regulation in the chick allantois. J Exp Zool. 1946;101:445-53.

초   록

미장은 장 발달의 과정 중, 가장 꼬리 쪽에 일시적으로 생기는 구조이다. 미장의 퇴화과정에서 문제가 생길 경우 꼬리창자낭종 및 꼬리퇴행증후군을 일으키는 것으로 알려져 있지만 언제 퇴화가 시작되어 끝나는 지나 분자적 특징과 메커니즘이 밝혀져 있지 않다. 따라서, 이 연구에서 조직학적으로 미장의 퇴화가 언제 시작되어 끝나는지 확인하였고, TUNEL 법을 사용하여 세포자멸사를 관찰하였다. 이로 인한 분자적 특징인 기저막의 퇴화를 확인하였고, 추정컨대 세포자멸사를 유도하는 분자적 경로를 제안하였다. 이를 통해, 인간 미장의 발생기전에 대한 이해를 높이고, 세포자멸사의 억제 실험 등을 통해 꼬리창자낭종 및 꼬리퇴행증후군의 발병기전에 대한 연구를 발전시킬 수 있다.

주요어 : 미장, 세포자멸사. 꼬리창자낭종, 꼬리퇴행증후군, 닭배자, 장 발달

학   번 : 2019-29542